B.V. Chirikov and V.V. Vecheslavov

ARNOLD DIFFUSION
IN LARGE SYSTEMS
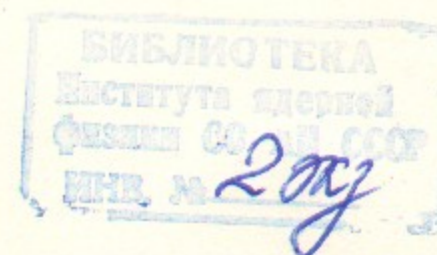
Budker INP 96-44
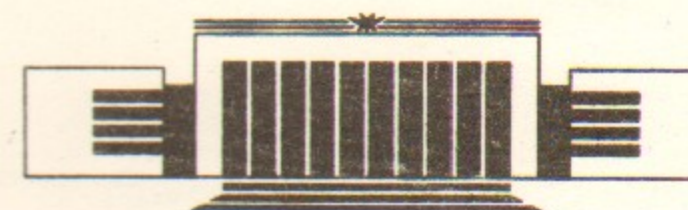
Arnold Diffusion in Large Systems

B. V. Chirikov and V. V. Vecheslavov

The State Research Center of Russian Federation
The Budker Institute of Nuclear Physics, SB RAS
630090, Novosibirsk 90, Russia

Abstract

The new regime of Arnold diffusion with a power-law dependence of the diffusion rate on perturbation strength was studied both theoretically and in numerical experiments. The theory developed predicts this new regime to be universal in the perturbation intermediate asymptotics, the latter being the wider the higher dimensionality of the perturbation frequency space, particularly, in large systems with many freedoms. The results of numerical experiments satisfactorily agree with the theoretical evaluations.

E-mail:chirikov@inp.nsk.su

1. Introduction: universal nonlinear instability

One of the most interesting phenomena in Hamiltonian dynamics is the so-called *Arnold diffusion* (AD), a peculiar universal instability of many-dimensional nonlinear oscillations [1,2]. This global instability had been predicted by Arnold [3] while its chaotic nature was discovered in Refs.[4,5,1] and further studied in detail in Refs.[6-11,14,15,17].

First, we briefly remind, following Ref.[17], the diffusion mechanism which is related to the interaction of nonlinear resonances. Consider a general Hamiltonian of many–dimensional oscillations:

$$H(I, \theta, t) = H_0(I) + \varepsilon \sum_{n,m} V_{nm}(I) \exp(in \cdot \theta + itm \cdot \Omega) \quad (1.1)$$

where I, θ are N-dimensional vectors of the action-angle variables; Ω is M-dimensional vector of driving frequencies; n, m are integer vectors of N and M dimensions, respectively, and ε stands for a small perturbation parameter. The dot in expressions like $n \cdot \theta$ denotes the scalar product. Below we shall consider a simpler case of the completely integrable and nondegenerate unperturbed system whose Hamiltonian $H_0(I)$ depends on the full set of N actions only.

Hamiltonian (nondissipative) dynamics is always determined by resonances (see, e.g., Refs.[1,2]) corresponding to particular terms in perturbation (1.1). The condition for a *primary resonance* with unperturbed frequencies (1.3) reads:

$$\omega_{nm} \equiv n \cdot \boldsymbol{\omega}(I) + m \cdot \Omega \approx 0 \quad (1.2)$$

In case of linear oscillations all the frequencies are fixed as parameters of the system which is either in or off resonance independent of initial conditions. However, for nonlinear oscillations with the action–dependent frequencies

$$\omega(I) = \frac{\partial H_0(I)}{\partial I} \qquad (1.3)$$

condition (1.2) determines resonance surfaces (zones) in the phase space that is the system is always in resonance for some initial conditions. On the other hand, nonlinearity stabilizes the impact of a (sufficiently weak) perturbation providing bounded oscillations even for resonant initial conditions. This is precisely due to *non–isochronous* oscillations (1.3). In one freedom such a nonlinearity is necessary and sufficient to destroy oscillation isochronism. A many–freedom generalization of that is the necessary condition for determinant

$$\left| \frac{\partial^2 H_0}{\partial I^2} \right| \neq 0 \qquad (1.4)$$

to be nonzero everywhere. In this case the system is called *nongenerated* which allows, particularly, the transformation from action to frequency space. In the latter, the resonance structure is especially simple and transparent as resonance surfaces (1.2) become planes.

Another condition for the nonlinear stabilization is the requirement for quadratic form of matrix $\partial^2 H_0/\partial I^2$ to be sign–definite or, geometrically, for surfaces $H_0(I) =$const to be convex [10]. The latter condition is a weaker one as it may include higher polynomial forms. Both conditions are sufficient only [10,11] but in physical applications it is unimportant restriction.

The above conditions ensure also the absence of the strong instability ($\sim \varepsilon$), due to a quasilinear (isochronous) resonance [1], especially when several (r) independent resonance conditions (1.2) are simultaneously satisfied. The latter is called *multiple (r-fold) nonlinear resonance*. However, a weak instability caused by nonresonant ($\omega_{nm} \neq 0$ for given initial conditions) terms in perturbation series (1.1) is possible, and it is just AD we are going to discuss in detail. Moreover, this weak instability is a typical phenomenon of nonlinear oscillations as it occurs under almost any, particularly arbitrarily weak, perturbation of a completely integrable system. The only restriction is the action space dimension d_a which must be larger than that of invariant torus ($d_a > d_t = 1$) [3]. The torus is absolute barrier for the motion trajectory which can only bypass it but never go through. For a driving perturbation ($M > 0$ in Eq.(1.1)) the minimal number of freedoms is, thus, $N_{min} = 2$ but in conservative case ($M = 0$) $N_{min} = 3$ as the trajectory is bound to follow an energy surface.

Even these minimal restrictions are not absolute being related to the *strong nonlinearity* only (1.4) when the effect of resonant perturbation is small ($\Delta I/I \sim \sqrt{\varepsilon} \ll 1$). In case of linear $H_0(I)$ (harmonic oscillator) N_{min} is less by one [12].

At least 3 perturbation terms in series (1.1) are necessary for AD. We shall call each of these terms a resonance (for the appropriate initial conditions of the motion). A single resonance retains the complete integrability of the unperturbed system. The interaction of 2 resonances already results in the formation of narrow *chaotic layers* around the unperturbed separatrices of both resonances [13–15]. Yet, the chaotic motion remains confined within a small domain of the layer. Only the combined effect of at least 2 *driving resonances* provides the diffusion along the layer of the first, *guiding*, resonance if $N \geq N_{min}$ (see Ref.[1] for details).

In the first approximation (1.2) the driving perturbation terms are non-resonant ($\omega_{nm} \neq 0$). Yet, the final effect is due to the *secondary resonances* between the driving perturbation and the slow *phase oscillation* on the guiding resonance. This is a particular case of the general rule that all the long-term effects in nonlinear oscillations are due to some resonances. For the problem in question the principal parameter is the ratio

$$\lambda = \frac{|\omega_{nm}|}{\omega_g} \qquad (1.5)$$

where $\omega_g \sim (\varepsilon \mid V_g \mid)^{1/2}$ is the frequency of small phase oscillations at the center of guiding resonance, and where V_g is the Fourier amplitude of the corresponding perturbation term. For a weak perturbation ($\varepsilon \to 0$) parameter $\lambda \gg 1$ is big, and thus the driving perturbation is a high-frequency one. In effect, this is equivalent to a low-frequency (adiabatic) perturbation. Hence the term *inversed adiabaticity* we use [14]. The symmetry between the standard and inversed adiabaticity is especially clear in a conservative system that is for the interaction of coupling resonances. Indeed, in this case the resonance interaction results in the energy exchange between the guiding and driving resonances. While for the former the perturbation is a high–frequency one (inversed adiabaticity), for the latter it is low–frequency (standard adiabaticity).

For an analytic perturbation the effect in both cases is exponentially small in *adiabaticity parameter* λ (1.5), namely [1,14]:

$$D \sim e^{-\pi\lambda} \sim w_s^2 \qquad (1.6)$$

where D is the local dimensionless diffusion rate in actions I within a chaotic

layer and where $w_s \sim |\Delta H_0|/\varepsilon V_g$ stands for the dimensionless layer width. Notice that effect (1.6) is of a nonperturbative nature as $\lambda \sim \varepsilon^{-1/2}$.

This is the simplest resonant mechanism of AD. In particular models the accuracy of such a 3-resonance approximation was found to be within a factor of 2 provided the perturbation was not too weak that is adiabaticity parameter λ is not very big [1] (see also Section 3 below).

As $\lambda \to \infty$ the higher-order resonances with $|n|,|m| \to \infty$ come into play. Even though their amplitudes $V_{nm} \sim \exp[-\sigma(|n|+|m|)]$ drop exponentially the detunings $|\omega_{nm}|$ also rapidly decrease. The operative resonances which control the diffusion has been roughly singled out in Refs.[1,15] by minimizing the expression

$$-\ln D \equiv E \sim k + \lambda(k) \gtrsim \lambda_0^{1/L} \qquad (1.7)$$

with respect to $k = |n| + |m|$; where $\lambda_0 = \omega_0/\omega_g$, ω_0 stands for a characteristic oscillation frequency, and the following diophantine estimate was used:

$$\omega_{nm} \sim \frac{\omega_0}{k^{L-1}} \qquad (1.8)$$

The most important parameter here

$$L = N + M - r \qquad (1.9)$$

is the number of linearly independent (incommensurate) unperturbed frequencies on an r-fold resonance. We shall call L the *resonance dimension* (in frequency space). Actually, Eq.(1.9) gives the maximal dimension when all L independent frequencies do contribute to the driving resonances which may be termed the *full resonances*. There are also *partial resonances* which depend on a smaller number of frequencies $\tilde{L} < L$. Even though the latter are just a few they are crucially important for the new AD regime which is the main subject of this paper (Section 5).

Estimate (1.7), which represents another AD mechanism, seems to agree with numerical data [7,14]. On the other hand, Nekhoroshev rigorously proved the upper bound of type (1.7) but with a different exponent [10] ($M = r = 0$):

$$L \le L_N = \frac{3(N-1)N}{4} + 2 \qquad (1.10)$$

Even for the minimal dimensions $N = 3$ this upper bound $L_{max} = 6.5$ considerably exceeds estimate (1.9): $L = 2$ ($r = 1$). The difference becomes increasingly large as $N \to \infty$. Even though this discrepancy is not a direct

contradiction as Eq.(1.10) is the upper bound it constitutes a problem: what would be the origin of the difference between the two estimates?

Recently, this problem has been resolved by Lochak [11] who rigorously proved a more efficient Nekhoroshev-type estimate with exponent (1.9) (for $M = 0$ but any r). The point is that Lochak assumed convexity of the unperturbed Hamiltonian $H_0(I)$ explained above whereas Nekhoroshev's proof holds under a weaker condition of the so-called steepness of H_0. From the physical point of view this difference appears to be insignificant. At least, we are not aware of any example of a steep but non-convex H_0.

Both the diffusion rate as well as the measure of chaotic component ($\sim w_s$, see Eq.(1.6)) are exponentially small in perturbation $\varepsilon \to 0$. Hence the term *KAM integrability* [14] referring to the Kolmogorov–Arnold–Moser theory which proves the complete integrability for most initial conditions as $\varepsilon \to 0$. Such a partial integrability, or better to say almost integrability, is as good as the approximate adiabatic invariance. Notice, however, that the complementary set of the initial conditions supporting AD - the so-called *Arnold web* - is everywhere dense as is the set of all resonances (1.2) anyone of which can be a guiding resonance. Also, the diffusion is exponentially slow in actions I only while the change in oscillation phase θ variation is much faster, with a characteristic time of the inversed Lyapunov exponent, namely: $(\delta\dot\theta) \sim \omega_g/|\ln w_s| \sim T_w^{-1}$ where T_w is the oscillation period in chaotic layer (see Eq.(2.2) below).

Both rigorous estimates are valid asymptotically, for sufficiently small ε only. For example, Lochak requires [11] ($L \gg 1$):

$$\varepsilon < \varepsilon_L \sim \left(\frac{\sigma^2}{L}\right)^{2L^2} \qquad (1.11)$$

This is very small perturbation, and the problem arises to estimate the diffusion rate in the *intermediate asimptotics*: $\varepsilon_L \ll \varepsilon \ll 1$, or $1 \ll \lambda_0 \ll \lambda_L$. This problem was first addressed in Refs.[14] where a new regime of diffusion, called the *fast Arnold diffusion* (FAD), was conjectured from some preliminary results of numerical experiments. Two peculiar characteristics of the new regime as contrasted to the *far-asymptotic* AD (1.11) are as follows:

(i) the dependence of the diffusion rate on adiabaticity (perturbation) parameter λ_0 (1.7) is a power law rather than exponential, and

(ii) the diffusion rate does not depend on resonance dimension L, particularly, on the number of freedoms N (cf. Eq.(1.7)).

Precisely these regularities have been observed in numerical experiments with another many–dimensional model [16]. However, the authors [16] have given a different interpretation of their numerical results. Instead, we tryed to agree the same results with our new diffusion mechanism [17]. Unfortunately, both interpretations remained somewhat ambiguous because the perturbation in those numerical experiments was not sufficiently small to reach any asymptotic behavior where the theoretical estimates were expected to hold true. To resolve this ambiguity we continued numerical and theoretical studies with the same model but at a much weaker perturbation. In this paper we report on our first results and present their theoretical explanation.

2. Model and numerical experiments

Following Refs.[16,17] we make use here of the same model with Hamiltonian

$$H(x, p, t) = \frac{|p|^2}{2} - K \sum_{i=1}^{N+1} \cos(x_{i+1} - x_i) \delta_1(t) \qquad (2.1)$$

and periodic boundary conditions ($x_{N+2} = x_1$; $p_{N+2} = p_1$) where p, x are action–angle variables, $\delta_1(t)$ stands for the δ–function of period 1, and $K \to 0$ is small perturbation parameter. Notice that the number of freedoms in this model can be reduced to N due to the additional motion integral $\sum p_i = const$. Unperturbed frequencies $\omega_i = p_i$ equal to the action variables, and energy surfaces $H_0(p) = |p|^2/2 = const$ are spheres, hence, strictly convex with unity determinant (1.4). The driving perturbation in the form of periodic "kicks" is not important for the diffusion but greatly simplifies numerical experiments as it allows to make use of a (many–dimensional) map rather than of differential motion equations.

Even though this model does not immediately represent by itself a physical system it is very convenient for the studies into subtle nonlinear phenomena like AD. The emerging theory can, then, be applied to some real physical problems, such as the stability of the Solar system [18] or of charged particles in magnetic fields of plasma devices, accelerators and colliding beams [15,19].

In previous works the diffusion in many–dimensional models like (2.1) was studied down to $K \sim 0.1$ only [16,9]. At such perturbation and large N a considerable part of phase space becomes globally chaotic which shadows the AD effect. Even though a combined action of AD and global diffusion is an interesting problem important for applications [1,15], here we wanted to understand, first of all, the mechanism of the proper AD. To this end we went down as far as to $K \sim 10^{-6}$ with number of freedoms up to $N = 15$. Realization of this program has required essentional modification of the problem itself. The point is that the direct computation of the diffusion rate quickly becomes prohibitively long as $K \to 0$, especially as a multiple computation precision is required for such a small K. To overcome this technical difficulty we have taken a different approach [14], namely, computing the chaotic layer width w_s and recalculating the diffusion rate from the relation like (1.6). Of course, this make any sence for the number of model's freedoms $N \geq N_{min}$ (Section 1). In this way we have managed to reach (for another model) the adiabaticity parameter value up to $\lambda_0 \approx 50$ with a routine computer as compared to $\lambda_0 \approx 10$ only for the direct diffusion calculation on CRAY supercomputer [7]. In model (2.1) this would roughly correspond to $K \sim \lambda^{-2} \sim 4 \times 10^{-4}$ and 10^{-2}, respectively, and $N = 2$ only.

In the present work we go further, and give up the calculation of diffusion rate altogether. Instead, we are studying numerically and developing the theory of the chaotic layer only. This proved to be sufficient to understand the mechanism of AD as well since both are essentially determined by the same higher–order adiabaticity parameter (1.5), and exponent in Eq.(1.7). Then, all we need in numerical experiments is computing the oscillation period $T(w_s)$ inside the chaotic layer of a guiding resonance, and recalculating layer width w_s using simple relations [1]:

$$\omega_g T_{min} = \ln \frac{32}{w_s}, \qquad \omega_g T_{av} = \ln \frac{32}{w_s} + 1 \qquad (2.2)$$

where T_{min}, T_{av} are the shortest and average periods, respectively. Both values are in a reasonable agreement: $< \ln(w_{min}/w_{av}) >= 0.31$ within the rms fluctuations $\Delta \ln(w_{min}/w_{av}) = \pm 0.39$, and both underestimate the full layer width. This is because the diffusion at the layer edge is very slow, so that 100 oscillation periods used in numerical experiments were insufficient to reveal the whole layer. A crude estimate [14] leads to the expected correction factor of the order of 2. No such correction was introduced into numerical data but it will be discussed below in Section 3.

A primary coupling resonance $\omega_1 \approx \omega_2$ with phase oscillation frequency $\omega_g = \sqrt{2K}$ has been chosen as the guiding resonance. Correspondingly, $p_1 \approx p_2 \approx p_g$ while other p_i ($i = 3, ..., N+1$) were taken at random ($mod\ 2\pi$). For the trajectory to be inside the layer the initial value of the guiding resonance phase was taken approximately $\psi_1 = x_1 - x_2 \approx \pi$. However, for small K the exact position of the layer had to be located numerically prior to w_s computation by a special searching part of the code. The computation was

8

9

performed for 7 values of $N = 2, 3, 4, 5, 7, 9, 15$ at the same initial conditions of a single trajectory.

The summary of results is presented in Figs.1 and 2. The lower bound of $w_s \sim 10^{-22}$ was determined by computation accuracy (about 30 decimal places). The values of the principal model parameter – the number of independent unperturbed frequencies, or the resonance dimension $L = N + M - r = N$ are also indicated. Notice that under particular conditions of numerical experiments the resonance dimension is equal to the number of model's freedoms because the driving perturbation is periodic ($M = 1$), and guiding resonance is simple ($r = 1$).

The most striking feature of the empirical data is a qualitatively different behavior in case of $L = 2$ which was observed already in Refs.[16]. The rest of data show no systematical dependence on L but rather big fluctuations which rapidly increase with λ.
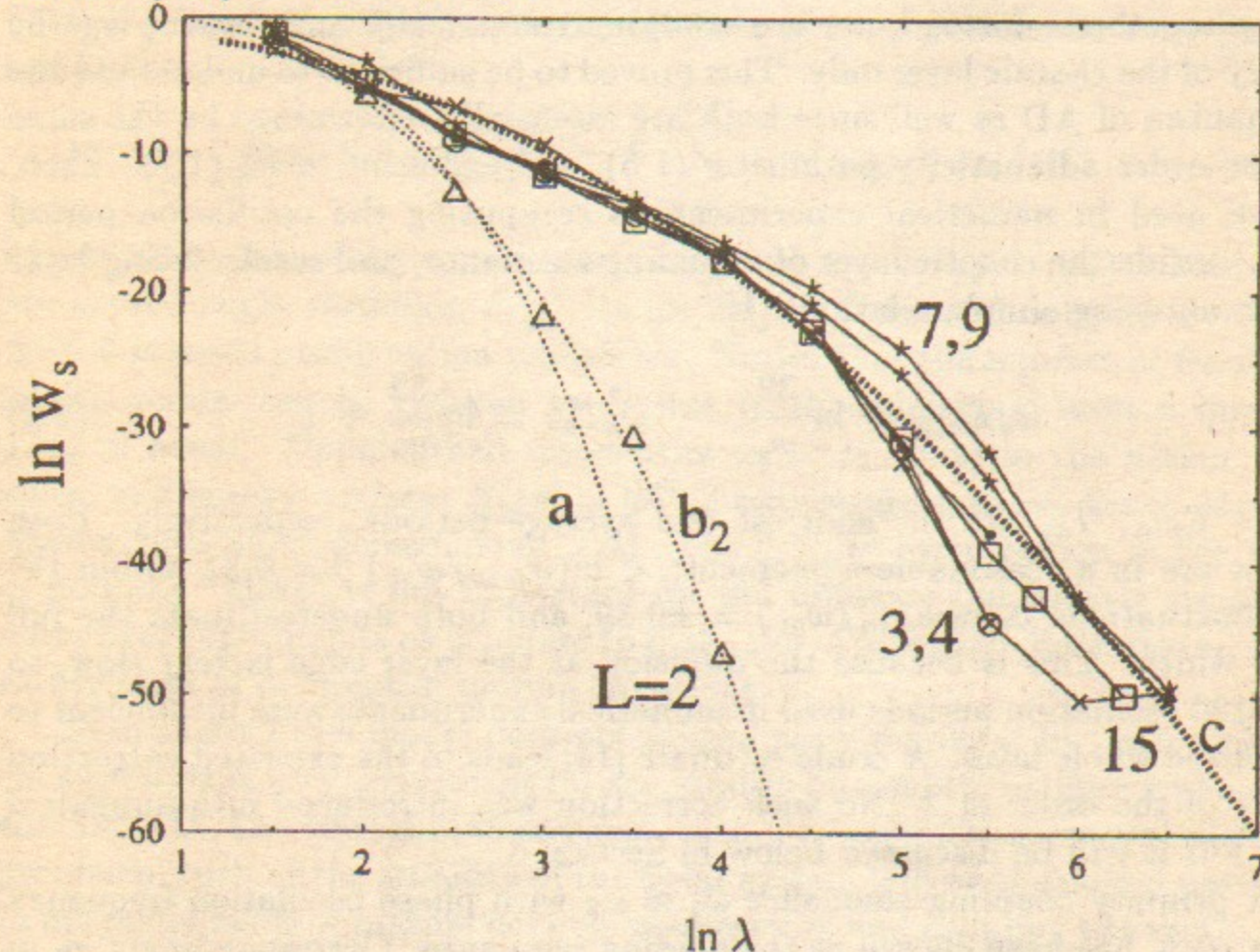

Fig. 1. Summary of numerical data for model (2.1). Broken solid lines connecting various symbols show computed values of w_s as a function of adiabaticity parameter $\lambda \equiv 1/\sqrt{K}$ and of resonance dimension $L = N$ indicated by numbers. Dotted lines represent the theory: (a) small–λ limit, 1 fitting parameter, Eq.(3.5); (b_2) large–λ limit for $L = 2$, 2 fitting parameters, Eq.(4.9); (c) intermediate asymptotics, 3 fitting parameters, Eq.(5.8).
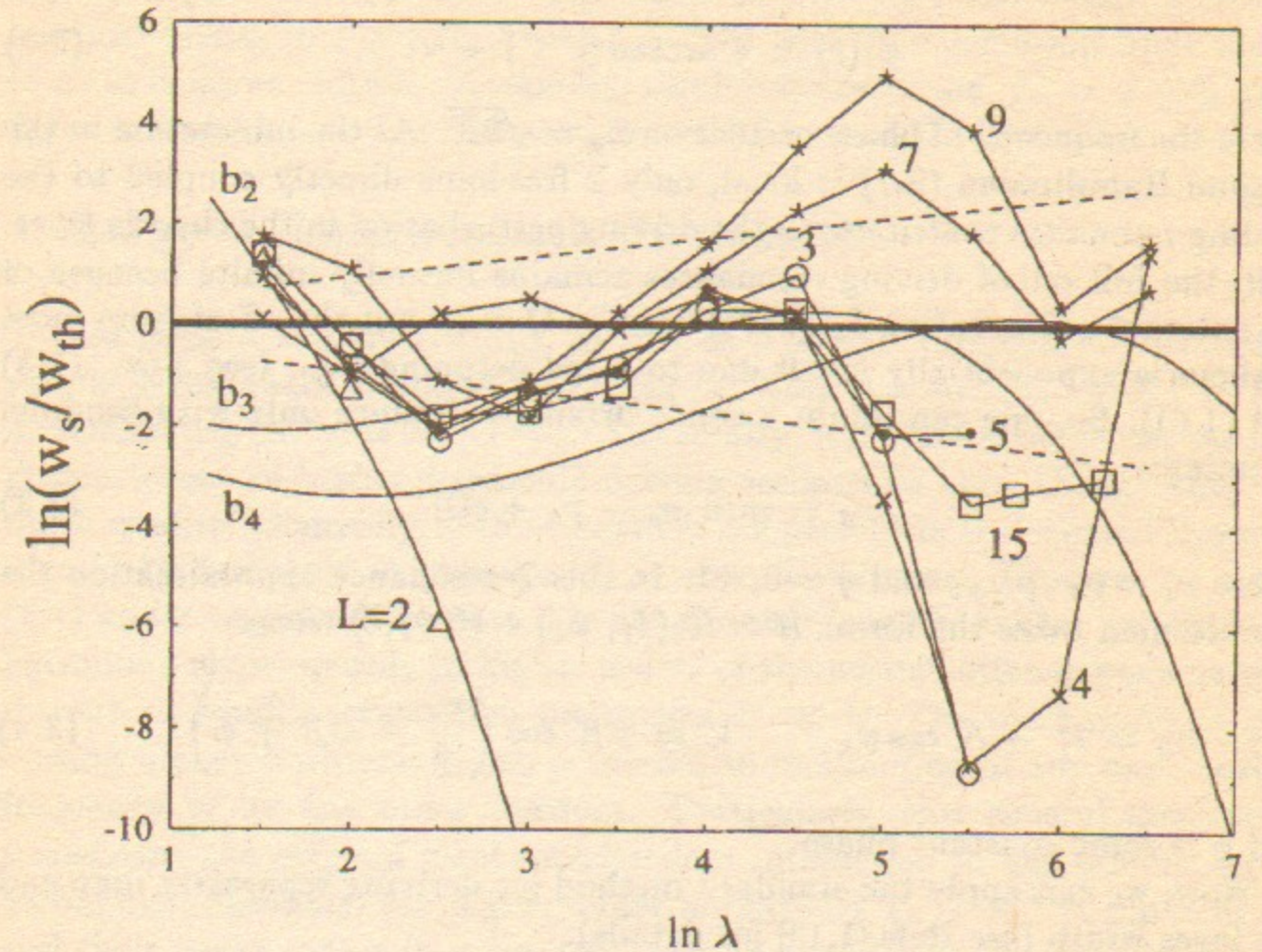

Fig. 2. The same data as in Fig.1 with respect to theoretical dependence $w_{th}(\lambda)$, Eq.(5.8) (curve c in Fig.1). Thin solid curves $b_{\tilde{L}}$ represent first 3 members of the family $w_s(\lambda, \tilde{L})$, Eq.(4.9) (cf. Fig.3). Two dashed lines show rms w_s fluctuations (5.11).

3. Small–λ limit: a simple dynamical theory

In the first approximation with respect to a small perturbation parameter K we can consider the primary driving resonances only which are explicitly present in the original Hamiltonian (2.1). Then, the problem is very similar to one studied in Ref.[1] apart from a different expression for the kinetic energy. First, we change variables for the two freedoms which determine the guiding resonance: $x_1, x_2, p_1, p_2 \rightarrow \psi_1, \psi_2, I_1, I_2$ where

$$\psi_1 = x_1 - x_2, \quad \psi_2 = x_1 + x_2, \quad p_1 = I_1 + I_2, \quad p_2 = I_2 - I_1, \quad (3.1)$$

In this approximation the momentum $I_2 \approx \dot{\psi}_2$, and all $p_i \approx \dot{x}_i$ for $i \geq 3$ are constant and determine the frequencies of driving resonances. The

unperturbed motion on the separatrix of the guiding resonance is given by

$$\psi_1(t) = 4 \arctan\left(e^{\omega_g t}\right) - \pi \qquad (3.2)$$

where the frequency of phase oscillation $\omega_g = \sqrt{2K}$. As the interaction in the original Hamiltonian (2.1) is local, only 2 freedoms directly coupled to the guiding resonance contribute to the driving perturbation in the chaotic layer. Still, the full set of driving resonances remains formally infinite because of the external perturbation $\delta_1(t)$ of frequency $\Omega = 2\pi$ but the effect from most of them is exponentially small due to large detuning ω_{nm} (see Eqs. (1.5) and (1.6)). So, one can retain a single driving resonance only with minimal detuning:

$$\omega_d = min \, |p_g - p_d + q\Omega| \qquad (3.3)$$

where $p_d = p_3$, p_{N+1} and $q = 0, \pm 1$. In this 2-resonance approximation the Hamiltonian takes the form: $H = H_0(I_1, \psi_1) + V(\psi_1, t)$ where

$$H_0 = I_1^2 - K \cos \psi_1, \qquad V \approx -K \cos\left(\frac{\psi_1}{2} - \omega_d t + \phi\right) \qquad (3.4)$$

and ϕ is some constant phase.

Now, we can apply the standard method for deriving separatrix map and the layer width (see Refs.[1,13] for details):

$$w_s = \frac{\Delta H_0}{K} \approx 4\pi f \lambda_0^2 e^{-\pi\lambda_0/2} \qquad (3.5)$$

where ΔH_0 is the layer width in energy, $\lambda_0 = \omega_d/\omega_g = \lambda\omega_d/\sqrt{2}$, and $\lambda \equiv 1/\sqrt{K}$. Besides usual approximations for such evaluations an additional factor $f \sim 1$ shows up for model (2.1) because the relative perturbation $|V/H_0| \sim 1$ is not small. In a particular case $N = 1$, which reduces to the well studied standard map, this factor $f \approx 2.15$ was found in numerical experiments [1], and later confirmed with a much better accuracy in Ref.[20]: $f = 2.255...$ The best theoretical value recently derived is $f \approx 2.14$ [21]. Uncertainty in this factor limits the theoretical accuracy of relation (3.5). Partly, it is balanced by an underestimated layer width, also by a factor of 2 [14] as discussed above. So, factor $f = f_{th}/f_n$ in Eq.(3.5) is actually the ratio of theoretical f_{th} to the correction $f_n = w_\infty/w_s$ of empirical w_s value (for 100 oscillation periods in our case) to obtain the true value w_∞ for infinitely many periods.

In this small–λ region the width w_s does not depend on N (Fig.1) because the original interaction is local. However, the size of this region is rather narrow. Comparison of numerical data for $L = 2$ with theory (3.5) (dotted line a) is presented in Fig.1. The value of $f = 0.64$ was obtained from 3 leftmost points in Fig.1 ($\ln\lambda = 1.5 - 2.5$) with rms deviation from theory (3.5) $\Delta \ln w_s = \pm 0.53$. Assuming empirical correction $f_n = 2$ [14] gives $f_{th} = 1.3$ which is rather different from that in the standard map.

4. Large–λ limit: statistical estimates

For large λ the layer width, as well as AD rate, progressively exceeds a simple 2–resonance estimate (3.5) (Fig.1). This was noticed already in first numerical experiments on AD [1]. Apparently, it is some strange, on the first glance, effect of higher–harmonic driving resonances even though they are much weaker. Generally, such resonances are present in the original Hamiltonian (1.1), and their amplitudes V_{nm} are explicitly given. However, in model (2.1) under consideration here it is not the case, and the higher perturbation harmonics show up only in higher orders of the perturbation expansion with respect to small perturbation parameter $K \ll 1$. The mechanism of generating higher–harmonic terms is related to modulation of any unperturbed frequency p_i by any other freedom. Particularly, this general mechanism transforms the original local interfreedom interaction in the system into a global one. Roughly, the higher–order amplitudes $V_n \sim K^n = \exp\left(n\ln K\right)$, and their decay rate σ (per freedom) can be assumed in the form [17]:

$$\sigma = \ln\frac{A}{K} \qquad (4.1)$$

with some constant A depending on a particular shape of the perturbation. In our model (2.1) the leading higher terms approximately correspond to $A \approx 2$ which we shall use below. Notice that the amplitudes do not depend on the external perturbation harmonic m as it is a δ–function.

A counterbalance to weaker higher perturbation terms is smaller λ (1.5) due to smaller detuning ω_{nm} (1.2). Generally, dependence $\omega_{nm}(n, m, \omega)$ is very complicated, with wild fluctuations, and exact evaluation of a higher–order perturbation is practically impossible and even useless beyond a few first terms [21]. However, the leading dependence can be singled out as follows (see, e.g., Refs.[22,23]):

$$\omega_{nm} = \frac{\Omega}{n^{L-1}} F_{nm}(\omega) \qquad (4.2)$$

where new function F_{nm} describes now the fluctuations only. The latter are quite big which is the main obstacle for reliable estimates. In some

special cases function $F_{nm} = F_0$ is simply a constant For example, in case of $L = 2$ and frequency ratio $R = \omega/\Omega = (\sqrt{5} - 1)/2$ ("the most irrational" real number): $1/F_0 = R + 1/R = \sqrt{5}$. Generally, only a sort of statistical estimates is possible by setting $F_{nm}(\omega) \approx F_f \approx const$ to some average or "most like" value to be fitted from numerical data.

Now, a particular term of the higher–order perturbation takes a form similar to Eq.(3.4):

$$V_n \sim e^{-n\sigma(L-1)} \cos\left(\frac{n\psi_1}{2} - \omega_{nm}t + \phi_{nm}\right) \qquad (4.3)$$

Here n is modulus of a single component of the integer vector, hence factor $(L - 1)$ which is less by one than the full number of frequencies because of δ–function in Hamiltonian (2.1) as discussed above. Assuming again that term (4.3) provides the main contribution to the formation of chaotic layer, which seems to be plausible owing to big detuning fluctuations, we arrive, similar to Eq.(3.5), at the following estimate for the layer width:

$$w_s \sim \left(\frac{2e\lambda_n}{n}\right)^n \exp(-E(n)) \qquad (4.4)$$

Here the principal exponent (cf. Eq.(1.7))

$$E(n) = n\sigma(L-1) + \frac{\pi\lambda_n}{2}, \qquad \lambda_n = \omega_{nm}/\omega_g \approx \lambda_0 \frac{F_f}{n^{L-1}} \qquad (4.5)$$

where $\lambda_0 = \frac{\Omega}{\omega_g} = \lambda\Omega/\sqrt{2}$, and $\lambda \equiv 1/\sqrt{K}$ (Fig.1).

The minimum of $E(n)$ equals to

$$E_{min} = \sigma^p L \Lambda^{1/L}, \qquad \Lambda = \frac{\pi^2}{\sqrt{2}} F_f \lambda, \qquad p = 1 - \frac{1}{L} \qquad (4.6)$$

and is reached at $n \approx n_0$ where

$$n_0^L \approx \frac{\Lambda}{\sigma}, \qquad \frac{\lambda_n}{n_0} \approx \frac{2\sigma}{\pi} \qquad (4.7)$$

The latter relation shows that the factor in Eq.(4.4) approximately reduces to a constant which renormalizes the amplitude decay rate: $\sigma \to \sigma_L$ where

$$(L - 1)\sigma_L \approx (L - 1)\sigma - \ln\sigma - \ln\frac{4}{\pi} - 1 > 0 \qquad (4.8)$$

The latter inequality is a necessary condition for validity of these approximate relations. This condition is satisfied for sufficiently large original σ, or small K (see Eq.(4.1)).

Finally, the approximate relation for the layer width in this limit reads:

$$\ln w_s \approx A_f - b(L)\sigma_L^p L\Lambda^{1/L} \qquad (4.9)$$

This theoretical dependence is also shown in Fig.1 (curve b_2) for $L = 2$ and fitted values $A_f = 5.42$, and $F_f = 0.34$ for the detuning parameter in Eq.(4.6). The rms deviation for 5 points ($\ln\lambda = 2 - 4$) is $\Delta \ln w_s = \pm 0.71$. While average detuning F_f has a reasonable value, the factor A_f seems too big (see next Section). Apparently, this discrepancy characterizes the accuracy of our statistical estimates. The additional parameter $b(L) = 1$ was set to unity for $L = 2$, and will be discussed in detail in Section 5 below.

For bigger L the behavior is completely different, and this is our most interesting result to be described in the next Section.

5. Intermediate asymptotics: Fast Arnold diffusion

The origin of a crucial change in dependence $w_s(\lambda)$ is related to factor $L - 1$ in expression for exponent $E(n)$ (4.5). The effect of this factor was previously missed in Refs.[1,15] (cf. Eq.(1.7)). Indeed, it leads to a non-monotonic dependence $w_s(L)$ according to Eq.(4.9). The latter was derived from optimization with respect to harmonic number n among the driving resonances with the maximal dimension $L = N$ only. Meanwhile, there are also resonances of lower dimension with $\tilde{L} < L$. So, we need the second optimization, now with respect to $\tilde{L}$, as was first done in Ref.[14] (see also Ref.[17]). First, we explain the idea of optimization for a simple example (cf. Eq.(4.9))

$$w_s = \exp(-L\lambda^{1/L}) \qquad (5.1)$$

The new factor L decreases the layer width as L grows, and thus counteracts the increase in w_s due to dependence $\lambda^{1/L}$. For any pair $L_1 < L_2$ there is a certain value of $\lambda = \lambda^*$ at which both w_s values coincide. Namely:

$$\lambda^* = \left(\frac{L_2}{L_1}\right)^{\frac{L_1 L_2}{L_2 - L_1}} \qquad (5.2)$$

If $\lambda < \lambda^*$ the value $w_s(L_1) > w_s(L_2)$ and vice versa. Thus, for a given λ the particular $\tilde{L}(\lambda)$ should be found which provides maximal w_s. In this way we would obtain a broken line which is the envelope of the family of

curves $w_s(\lambda, \tilde{L})$. Interestingly, the existence of such a family of intersecting curves could be inferred already (but was missed) from the validity of the 2-resonance approximation [1,2,6,7] which corresponds to $\tilde{L} = 1$.

For $L \gg 1$ a smooth approximation to the envelope is found from the local condition

$$\frac{dw_s}{d\tilde{L}} = -w_s \, \lambda^{1/L} \left(1 - \frac{\ln \lambda}{\tilde{L}}\right) = 0 \qquad (5.3)$$

Whence optimal

$$\tilde{L}_0(\lambda) = \ln \lambda \qquad (5.4)$$

and

$$w_{max}(\lambda) = w_s(\tilde{L}_0) = \lambda^{-e} \qquad (5.5)$$

where $e = \exp(1)$. Thus, the dependence of the layer width on adiabaticity parameter becomes a *power law* provided $\tilde{L}_0 \leq L$, or

$$\lambda \leq \lambda_L = e^L \qquad (5.6)$$

that is for a not-too-weak perturbation. This border is, of course, much higher (in ε) than that in the rigorous theory (cf. Eq.(1.11)). We term region (5.6) the *intermediate asymptotics* as contrasted to the *far asymptotics* for the reversed inequality. The former is always bounded from above but rapidly grows with L, and may be arbitrarily large as $L \to \infty$.

We call this regime the *fast Arnold diffusion* (FAD). Within domain (5.6) the layer width (and diffusion rate) does not depend on L but asymptotically, for any fixed L and $\lambda \to \infty$, the Nekhoroshev-like dependence (4.9) is recovered.

In Fig.3 the power–law mechanism is illustrated, for a simple example (5.1), by plotting a family of curves $\ln\left(w_s(\lambda, \tilde{L})/w_{max}\right)$ which are touching the line of maximal $w_{max}(\lambda)$ (5.5) up to the largest $\tilde{L} = L = 5$.

For a more realistic asymptotic relation (4.9) the optimization is more complicated because of the additional dependence on L via σ_L^p. Partly, that can be removed by approximate renormalization: $\Lambda_0 \to \Lambda_0/\sigma$. For $L \gg 1$ the remaining dependence (4.8) is weak and can be neglected, at least in evaluating optimal $\tilde{L}_0$, which now becomes (cf. Eq.(5.4)):

$$\tilde{L}_0(\lambda) \approx \ln\left(\frac{\Lambda}{\sigma}\right) \qquad (5.7)$$

However, we retain a more accurate σ_L (4.8) in the final expression:
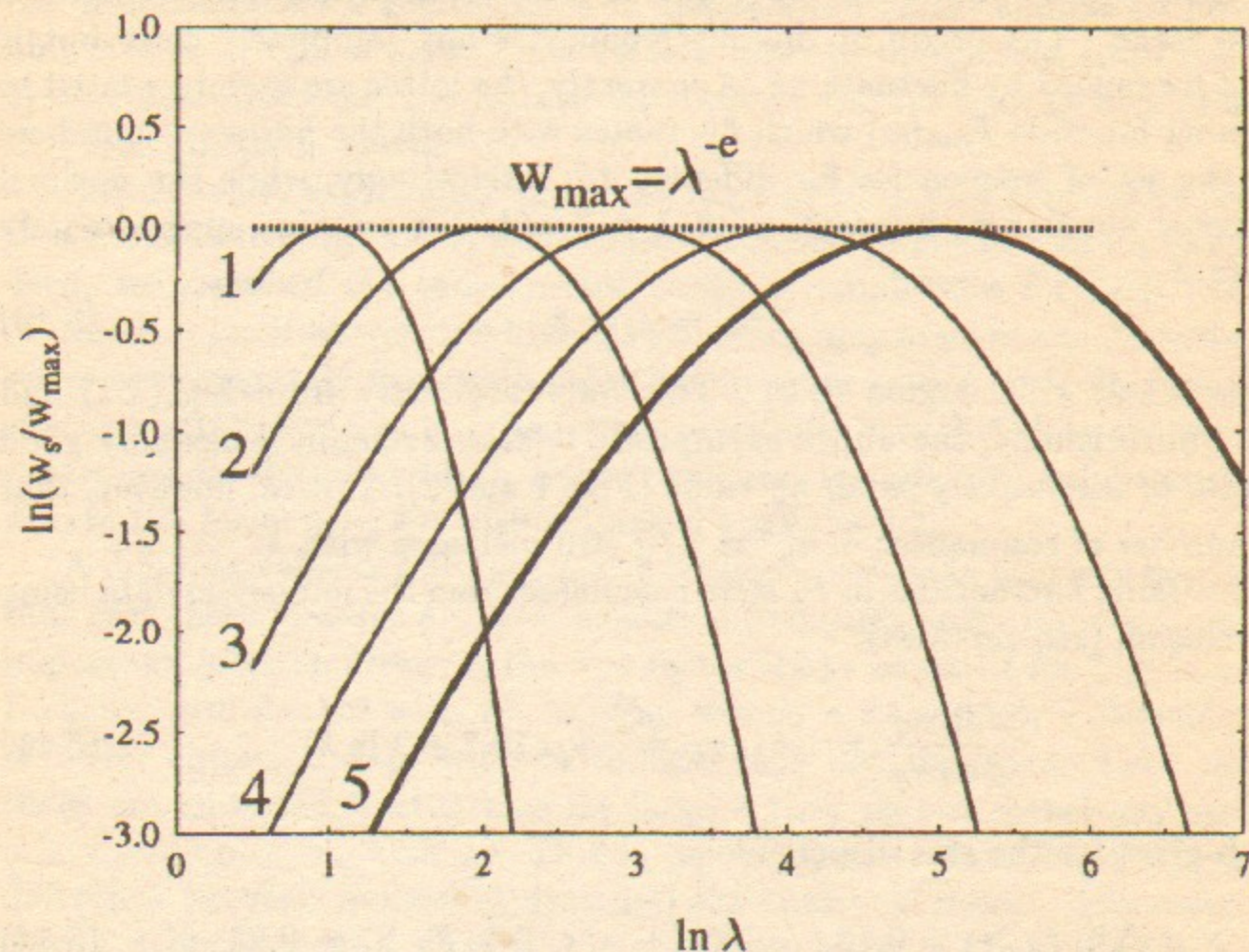
Fig. 3. A scheme of the family $w_s(\lambda, \tilde{L})$, Eq.(5.1), for $\tilde{L} = 1 - 5$ as indicated, with maximal $\tilde{L} = L = 5$ which form a smooth power–law dependence (5.5) shown by dotted straight line.

$$\ln w_s \approx A_f - b_f \, e \left[\sigma \ln\left(\frac{\Lambda}{\sigma}\right) - \ln\left(\frac{4\sigma}{\pi}\right) - 1\right] \qquad (5.8)$$

which is the main result of our studies. It is compared with numerical data in Fig.1 (curve c, see also Fig.2). Besides two fitting parameters previously used in Eq.(4.9) (curve b_2 in Fig.1), which now take somewhat different values: $A_f = -1.05$, and $F_f = 0.4$, we have to introduce the third one: $b_f = 0.29$. The fitting of empirical data has been performed for $N = 5, 7, 9, 15$ only. We excluded data for $N = 3, 4$ as they seem to violate condition (cf. Eq.(5.6))

$$\Lambda \leq \Lambda_L = \frac{\pi^2}{\sqrt{2}} F_f \, \lambda_L \approx \sigma \, e^L \qquad (5.9)$$

for $\ln \lambda \gtrsim 5$ (see Figs.1 and 2). Using the above fitted value for $F_f = 0.4$, and Eq.(4.1) for $\sigma = \ln(2/K) = \ln(2\lambda^2)$ we obtain from Eq.(5.9): $\ln \lambda_3 \approx 4.2$,

and $\ln \lambda_4 \approx 5.5$. While the first value is close to empirical one, the second is too large. The origin of this discrepancy is not completely clear but it might be caused by fluctuations. Apparently, the latter are mainly related to detuning function $F_{nm}(\omega)$ which fluctuates with both the harmonic numbers and the set of frequencies for different L. Interestingly, while the optimal harmonic number n_0 increases with $\lambda > \lambda_L$ (4.7) it remains approximately constant

$$n_0 \approx e \approx 3 \qquad (5.10)$$

in the whole FAD region (5.9). This follows directly from Eqs.(4.7) and (5.7). Surprisingly, the above asymptotic relations remain reasonably good in spite of a relatively small n_0 value (Figs.1 and 2). Notice, however, that the number of resonances $\sim n_0^{\tilde{L}_0} = \Lambda/\sigma$ still increases with λ.

Detuning fluctuations in F_f were calculated from the numerical data using the relation (see Eq.(5.8)):

$$\frac{d \ln w_s}{d \ln F_f} = -b_f e \sigma_L \approx -b_f e \,(0.7 + 2 \ln \lambda) \qquad (5.11)$$

which gives for the rms dispersion:

$$<\Delta \ln F_f>_4 = 0.18, \qquad \text{and} \qquad <\Delta \ln F_f>_6 = 0.25 \qquad (5.12)$$

The first value is the average over 4 cases with $N = 5, 7, 9, 15$ as in the main fitting; for the second $N = 3, 4$ are also included. The latter value is used in Fig.2 for rms fluctuations $\Delta \ln w_s$ according to Eq.(5.11).

The accuracy of our theory does not allow for a reasonable estimate of factor $A_f \approx -1$ in the main relation (5.8) whose value is considerably smaller as compared to $A_f \approx 5$ in Eq.(4.9). However, the value of a new fitting parameter $b_f = 0.29$, which we had to introduce in Eq.(5.8) instead of $b(2) = 1$ in Eq.(4.9), is a problem for the theory. It is impossible to fit the data for large L with the latter value nor vice versa that is with $b(2) = 0.3$, as in Eq.(5.8) but for $L = 2$, unless one assumes in Eq.(4.9) the value $F_f = 3$ instead of 0.3 which seems too big. In any event, something happens upon transition from $L = 2$ to $L \geq 3$ which is obvious from the data in Fig.1. To reconcile these data with the above theory one needs to assume a jump either in parameter b from 1 to 0.3 (with approximately the same $F_f \approx 0.4$) or in parameter F_f from 3 to 0.4 (with approximately the same $b \approx 0.3$ still to be explained anyway). Actually, the value $F_f = 3$ for $L = 2$ would contradict the rigorous upper bound $F_f \leq 1$ [22]. So, we have to understand the first possibility above.

In Ref.[17], using a somewhat different approach, the following expression has been derived for parameter b in the relation (2.11) similar to Eq.(5.8) above: $b \approx 1/\pi\sqrt{e} = 0.19$. This value is close to the present empirical one: $b_f = 0.29$. However, the former does not fit the far asymptotics (4.9) for $L = 2$ as discussed above.

A qualitative explanation of the decrease in $b(L)$ with L could be related to some underestimation of perturbation Fourier amplitudes in Eq.(4.3). Indeed, we assumed the independent decay of amplitudes for each freedom (factor $L - 1$). However, the higher harmonics may arise in the perturbation series not separately from each other but in some groups, thus decreasing an effective parameter L or σ. The former possibility is excluded by the assumed expression for detuning (4.2). Hence, we guess the effective amplitude decay rate in the form: $\sigma \to b \sigma$ with empirical $b \approx b_f \approx 0.3$.

A different value of $b = 1$ for $L = 2$ is also explained in this way because in that case there remains a single oscillation frequency only. However, another important question arises: is the new factor $b(L)$ a constant for $L \geq 3$ or does it change still further with L? In other words, is FAD really independent of N? Our empirical data seem to confirm such independence. Even though there are quite big fluctuations for large λ they do not reveal any systematic variation of w_s with L. This is especially clear from Fig.2 where the difference between numerical data and the theory is shown. Moreover, the theory explains even a small dip in the dependence $w_s(\lambda)$ around $\ln \lambda = 3$. This results from a deviation of the approximate smoothed envelope (5.8) from the family of curves $w_s(\lambda, \tilde{L})$, three of which are shown in Fig.2 (for $\tilde{L} = 2, 3, 4$, cf. Fig.3) as calculated from Eq.(4.9) with factor $b(2) = 1$, and $b(3) = 0.29$.

If the above hypothesis is true a new fitting is required as renormalization $\sigma \to b \sigma$ would result in more complicated expressions than just a single factor in Eqs.(5.8) and (4.9). By doing so we have found that the change in dependence $w_s(\lambda)$ according to Eq.(5.8) was negligible at the expense of some changes in the fitting parameters: $A_f = -0.88$, $b_f = 0.28$, $F_f = 0.21$ which appear to be reasonable also. A larger change $\delta A_f \approx 1$ occurs in the family of curves, Eq.(4.9), for $\tilde{L} > 2$, and their agreement with smooth envelope (5.8) becomes more poor owing to approximate relation (5.7). To keep the above estimates more self-consistent we neglect all these minor changes, and retain the above relations with a single parameter $b_f = 0.29$ for $L > 2$. In any event, the relations, being approximate any way, are much simpler in this form.

Interestingly, a half of the data in Fig.1 ($\ln \lambda \leq 4$, $L > 2$) fits also a simple

power law with exponent 6.3 which is very close to the value 6.6 obtained in Refs.[16,17] around $\ln \lambda \approx 2$. However, for larger $\ln \lambda > 4$ the deviation from such a simple dependence (it would be a straight line in Fig.1) progressively increases in accordance with theory (5.8).

6. Discussion

We have performed detailed studies into a new regime of AD - *the fast Arnold diffusion* - when the diffusion rate depends on the perturbation strength $\varepsilon = K$, for model (1.1) and (2.1) respectively, or on the adiabaticity parameter $\lambda \sim 1/\sqrt{\varepsilon} \sim 1/\sqrt{K}$ as a *power law* (5.8) rather than an exponential like Eq.(4.9).

We made use of a specific model (2.1) which is relatively simple and very convenient for numerical experiments with arbitrary number of freedoms N but, at the same time, is rather difficult for theoretical analysis. This is because the model represents the limiting case of the local interfreedom interaction. And not only 2-freedom one, which would model a pair interaction in a broad class of physical systems, but is even further restricted to the coupling with two nearest neighbor freedoms in a chain only. Moreover, the coupling is harmonic, so that only 3-frequency primary resonances (those for the two freedoms and for the driving perturbation) with harmonic numbers $n = \pm 1$ show up in the original Hamiltonian (2.1) independent of N. As a result, the higher-harmonic multifrequency resonances, which make the principal contribution to AD, arise in higher-order perturbation terms only which makes the theory very difficult from the beginning. We circumvented this difficulty by a plausible and simple conjecture (4.1) for the decay rate of the high-order perturbation amplitudes. However, to agree the empirical data with the theory we had, later on, to father modify this conjecture by introducing additional factor $b(L)$ in our main relations (4.9) and (5.8). Even though we suggest in Section 5 a qualitative explanation for $b(L) \neq 1$, the origin of this additional dependence remains as yet not completely clear, and it constitutes an open question in our theory. Apparently, this is related to a specific Hamiltonian (2.1) as discussed above.

Factor $b = 0.29$, assumed to be constant for $L = N > 2$, is one of the three fitting parameters in our main theoretical relation (5.8) for the FAD. As explained in Section 2 we actually computed and calculated the chaotic layer width w_s related to the diffusion rate via estimate (1.6). The second fitting parameter $F_f = 0.4$, which describes detuning fluctuations ω_{nm} (1.2),

also cannot be evaluated in the present state of the theory but was found numerically to be of a plausible value. Finally, the third fitting parameter A_f remains completely out of the theoretical reach, and it simply characterizes a global accuracy of the theory developed. We remind that all our estimates but the simplest one (3.5) are of a statistical nature owing to large detuning fluctuations. Within this accuracy and fluctuations the agreement between empirical data and the theory as presented in Figs.1 and 2 can be considered as satisfactory, especially taking into account a big range of w_s variation which comprises almost 22 orders of magnitude!

Surprisingly, all this huge range correspond to the intermediate asymptotics ($1 \ll \lambda \ll \lambda_L$, see Eq.(5.9)) with FAD, starting already from a relatively small $L = N \geq 5$. Even for $L = 3$ and 4 the FAD range is apparently of a comparable size, and only for the minimal $L = 2$ the far (exponential) asymptotics ($\lambda \gg \lambda_L$) clearly shows up. As already discussed in Section 5 a sharp change in dependence $w_s(\lambda)$ from $L = 2$ to $L = 3$ is precisely due to "misterious" factor b which drops by a factor of 3. Unfortunately, this does not allow to reach the far asymptotics, and to confirm the exponential dependence on N (4.9) for $\lambda > \lambda_L$ beyond minimal $L = 2$. Meanwhile, this would be important to decide on a different interpretation of N-independent diffusion for large N in Ref.[16]. The latter authors conjectured that such an independence is a result of the local interaction in model (2.1). This is contrary to our theory but not as yet to the direct empirical evidence. At the moment we can only remark that their reference to Wayne's theory [24] for the same model is irrelevant. Indeed, Wayne proved a long N-independent stability for very special, *nonresonant*, initial conditions (theorem 1.1) while AD occurs within chaotic layers only, that is also for highly specific but *resonant* initial conditions. Thus, the former theory is related to a global chaos rather than to KAM integrability with its peculiar Arnold web of chaotic layers.

In case of a global interaction (1.1) with strong nonlinearitry (1.4) and uniform amplitude decay rate our theory remains valid, and even becomes simpler as $\sigma = const$. However, the numerical experiments would be much more difficult for large N. On the other hand, both the FAD range (5.9) as well as the diffusion rate there depends generally on the number of incommensurate unperturbed frequencies $L = N + M - r$ (1.9) which may be large at the expense of large M, the number of driving perturbation frequencies.

Fast Arnold diffusion should not be confused with even much faster diffusion in degenerate systems or those with nonconvex energy surfaces (Section 1). In the latter case the diffusion mechanism is of a completely different nature. Apparently, this sort of diffusion was recently observed in numerical

experiments with the classical model of the Hydrogen atom in crossed electric and magnetic fields [25].

In the present study we have chosen one of the strongest primary resonance as guiding, with amplitude $V_g = V_1 \sim K$ (Section 2). In case of a high–harmonic guiding resonance ($V_g = V_n$, $n \gg 1$) the main effect would be tremendous drop in the diffusion rate due to exponential rise of the adiabaticity parameter with n (see Eq.(4.5)):

$$\lambda(n) \sim \exp\left(\frac{\sigma}{2}Ln\right) \sim \exp\left(\frac{\sigma}{2}L\rho^{1/L}\right) \qquad (6.1)$$

where $\rho(n) \sim n^L$ is the density of the guiding resonances in the Arnold web with harmonic numbers up to n (cf. Eq.(4.2)). Hence, the diffusion rate in the intermediate asymptotics drops exponentially with n or ρ, Eq.(5.8), and even as a double exponential in the far asymptotics!

Similar to Eq.(5.8) the resonance density $\rho(\lambda)$ calculated from Eq.(6.1) can be optimized with respect to intermediate $\tilde{L} \leq L$ to obtain the estimate:

$$\rho(\lambda) \sim \begin{cases} \lambda^{2/e\sigma}, & \lambda \leq e^{e\sigma N} \\ \left(\frac{2\ln\lambda}{\sigma N}\right)^N, & \lambda \geq e^{e\sigma N} \end{cases} \qquad (6.2)$$

The discussion of transport properties of the Arnold web can be found in Ref.[1].

In conclusion, our present studies confirm the previous conjecture and preliminary empirical data [14,17] concerning a new regime of fast Arnold diffusion. Moreover, we have found that in many–frequency ($L \gg 1$), particularly, large ($N \gg 1$) systems the FAD range in perturbation (5.9) is fairly big, so that this regime appears to be a typical one, in a sense, and might be important in various applications.

References

[1] B.V. Chirikov, Phys. Reports **52**, 263 (1979).

[2] A. Lichtenberg and M. Lieberman, *Regular and Chaotic Dynamics*, Springer (1992).

[3] V.I. Arnold, Dokl. Akad. Nauk SSSR **156**, 9 (1964).

[4] B.V. Chirikov, Studies in the Theory of Nonlinear Resonance and Stochasticity, preprint INP-267, Novosibirsk, 1969 (Engl. trans., CERN Trans, 71–40, 1971).

[5] G.V. Gadiyak, F.M. Izrailev and B.V. Chirikov, Proc. 7th Intern. Conf. on Nonlinear Oscillations (Akademie–Verlag, Berlin, 1977), Vol. II,1, p. 315.

[6] J. Tennyson, M. Lieberman and A. Lichtenberg, AIP Conf. Proc. **57**, 272 (1979); M. Lieberman, Ann. N.Y. Acad. Sci. **357**, 119 (1980).

[7] B.V. Chirikov, J. Ford and F. Vivaldi, AIP Conf. Proc. **57**, 323 (1979).

[8] T. Petrosky, Phys. Rev. A **29**, 2078 (1984).

[9] B. Wood, A. Lichtenberg and M. Lieberman, Physica D **71**, 132 (1994).

[10] N.N. Nekhoroshev, Usp. mat. nauk **32**, #6, 5 (1977).

[11] P. Lochak, Phys. Lett. A **143**, 39 (1990); Usp. mat. nauk **47**, #6, 59 (1992); P. Lochak and A. Neishtadt, CHAOS **2**, 495 (1992).

[12] A.A. Chernikov, R.Z. Sagdeev and G.M. Zaslavsky, Physica D **33**, 65 (1988); A. Lichtenberg and B. Wood, Phys.Rev. A **39**, 2153 (1989); B.V. Chirikov and V.V. Vecheslavov, The Structure of a Weakly Nonlinear Resonance, in: *From Phase Transitions to Chaos*, Eds. G. Györgyi et al, World Scientific, 1992, p. 273.

[13] N.N. Filonenko, R.Z. Sagdeev and G.M. Zaslavsky, Nuclear Fusion **7**, 253 (1967); G.M. Zaslavsky and N.N. Filonenko, Zh.Eksp.Teor.Fiz. **54**, 1590 (1968); G.M. Zaslavsky, B.V. Chirikov, Usp.Fiz.Nauk **105**, 3 (1971); A. Rechester and T. Stix, Phys.Rev.Lett. **36**, 587 (1976); D. Escande, Phys.Reports **121**, 163 (1985); V.F. Lazutkin, Dokl.Akad.Nauk SSSR **313**, 268 (1990); V.V. Afanasiev et al, Phys.Lett. A **144**, 229 (1990).

[14] B.V. Chirikov and V.V. Vecheslavov, How Fast is the Arnold Diffusion? Preprint INP 89–72, Novosibirsk, 1989; B.V. Chirikov and V.V. Vecheslavov, KAM Integrability, in: *Analysis etc*, Eds. P. Rabinowitz and E. Zehnder (Academic Press, 1990), p. 219.

[15] B.V. Chirikov, Fiz. Plasmy **4**, 521 (1978); Proc.Roy.Soc.Lond. A **413**, 145 (1987).

[16] K. Kaneko and T. Konishi, Phys. Rev. A **40**, 6130 (1989); T. Konishi, Suppl. Prog. Theor. Phys. **98**, 19 (1989); T. Konishi and K. Kaneko, J. Phys. A **23**, L715 (1990).

[17] B.V. Chirikov and V.V. Vecheslavov, J.Stat.Phys. **71**, 243 (1993).

[18] *Resonances in the Motion of Planets, Satellites and Asteroids*, Eds. S. Ferraz–Mello and W. Sessin, Univ. de Sao Paulo, Brazil, 1985; J. Wisdom, Icarus **72**, 241 (1987); J. Laskar, Nature **338**, 237 (1989); Icarus **88**, 266 (1990); Astron.Astrophys. **287**, L9 (1994).

[19] B.V. Chirikov, Priroda, 1982, #7, p.15; *Nolinear Dynamics Aspects of Particle Accelerators*, Lecture Notes in Physics Vol. 247, Springer, 1986; A. Lichtenberg, Phys.Fluids B **4**, 3132 (1992).

[20] V.F. Lazutkin et al, Physica D **40**, 235 (1989).

[21] V.V. Vecheslavov, Zh.Eksper.Teor.Fiz. **109** #5 (1996).

[22] A.Ya. Khinchin, *Continued fractions*, Fizmatgiz, Moskva, 1961 (in Russian); J. Cassels, *An Introduction to Diophantine Approximation*, Cambridge University Press, 1957; W. Schmidt, *Diophantine Approximations*, Lecture Notes in Mathematics **785**, Springer, 1980.

[23] B.V. Chirikov, Chaos, Solitons and Fractals **1**, 79 (1991).

[24] E. Wayne, Comm.Math.Phys. **104**, 21 (1986).

[25] J. von Milczewski, G. Diercksen and T. Uzer, Phys.Rev.Lett. **76**, 2890 (1996).